Acta Crystallographica Section F
Structural Biology and Crystallization Communications
ISSN 1744-3091

Crystallization and preliminary X-ray studies of an electron-transfer complex of ferredoxin and ferredoxin-dependent glutamate synthase from the cyanobacterium *Leptolyngbya boryana*

Kanako Shinmura, Norifumi Muraki, Ayako Yoshida, Toshiharu Hase and Genji Kurisu*

Institute for Protein Research, Osaka University, 3-2 Yamadaoka, Suita, Osaka 565-0871, Japan

Correspondence e-mail: gkurisu@protein.osaka-u.ac.jp

Received 11 January 2012
Accepted 26 January 2012

Ferredoxin (Fd) dependent glutamate synthase (Fd-GOGAT) is a key enzyme involved in nitrogen assimilation that catalyzes the two-electron reductive conversion of Gln and 2-oxoglutarate to two molecules of Glu. Fd serves as an electron donor for Fd-GOGAT and the two proteins form a transient electron-transfer complex. In this study, these two proteins were cocrystallized using the hanging-drop vapour-diffusion method. Diffraction data were collected and processed at 2.65 Å resolution. The crystals belonged to space group $P4_3$, with unit-cell parameters $a = b = 84.95$, $c = 476.31$ Å.

1. Introduction

Ferredoxin (Fd) is a one-electron carrier protein that contains a [2Fe–2S] cluster and is the sole major acceptor of electrons in the photosynthetic electron-transport system in oxygenic photosynthetic organisms. Fd transfers electrons from the donor side of photosystem I to multiple redox enzymes in cyanobacteria and chloroplasts. These include (but are not restricted to) Fd:NADPH oxidoreductase (FNR), nitrite reductase (NiR), sulfite reductase (SiR), glutamate synthase (glutamine 2-oxoglutarate amidotransferase; Fd-GOGAT) and Fd:thioredoxin reductase (FTR) (Hase *et al.*, 2006).

Based on the structures of the electron-transfer complexes Fd–FNR (Kurisu *et al.*, 2001), Fd–FTR (Dai *et al.*, 2007) and Fd–SiR (Saitoh *et al.*, 2006), which have been studied by X-ray crystallography and NMR, the current model of the interaction of Fd with a partner enzyme can be summarized as follows. An initial complex is formed by the interaction of (predominantly negatively) charged residues on Fd with (predominantly positively) charged residues on partner enzymes. Following this, exclusion of water from the hydrophobic interface between the two proteins stabilizes the complex. The interaction is not very strong ($K_d \simeq 10\ \mu M$) and depends partly on the salt bridges and partly on the topography of the noncharged and/or hydrophobic surfaces (Sakakibara *et al.*, 2012). The nature of the interprotein electron-transfer reaction demands that Fd and its various redox partners must interact and dissociate coordinatedly to allow multiple catalytic events to occur productively.

Fd-GOGAT is the largest of these Fd-dependent enzymes, with a molecular mass of 160 kDa. This enzyme contains FMN and a [3Fe–4S] cluster and catalyzes the two-electron reductive transfer of the amido group of Gln to 2-oxoglutarate (2-OG; Suzuki & Knaff, 2005). Pyridine nucleotide-dependent GOGAT is also present in a wide variety of organisms (Vanoni *et al.*, 2005). Eubacteria contain NADPH-GOGAT, which is composed of α and β subunits with molecular masses of 150 and 50 kDa, respectively; the α subunit corresponds to Fd-GOGAT and the β subunit is a flavoenzyme with two FADs and two [4Fe–4S] clusters. The pyridine nucleotide-dependent GOGATs found in oxygenic photosynthetic organisms are NADH-dependent enzymes. Cyanobacterial NADH-GOGAT has the two-subunit structure, while plant NADH-GOGAT is formed of a single long polypeptide with the two subunits fused. The three-dimensional structures of Fd-GOGAT from *Synechocystis* sp. PCC 6803 (van den Heuvel *et al.*, 2002) and of the α subunit of NADPH-

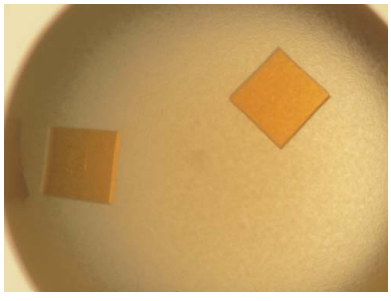

GOGAT from *Azospirillum brasiliense* (Binda *et al.*, 2000) are known. The overall polypeptide folding and the topology of the active sites are quite similar in these two GOGATs, indicating that their catalytic mechanism is the same or similar. The structures of the Fd–Fd-GOGAT complex and of the whole NADH-GOGAT remain to be elucidated.

We have cloned the genes for Fd-GOGAT and NADH-GOGAT from the cyanobacterium *Leptolyngbya boryana* (Okuhara *et al.*, 1999) and have been studying the structural and functional characteristics of these two GOGATs. In particular, the structure of the electron-transfer complex will give us an important insight into the mechanism of protein–protein interaction and electron transfer between Fd and Fd-GOGAT. Here, we report the crystallization of the complex of Fd and Fd-GOGAT and the preliminary results of X-ray crystal structure analysis.

2. Materials and methods

2.1. Protein expression and purification

Fd from *L. boryana* was prepared as described previously (Matsumura *et al.*, 1999; Kimata-Ariga *et al.*, 2000). To prepare mature Fd-GOGAT, a DNA fragment encoding the N-terminal part of Fd-GOGAT without the propeptide was amplified by PCR with the pair of primers P3 (5′-ACG**ACATGT**GTGGAGTTGGTTTTATTGTC-3′) and P4 (5′-GAGTT**GCC**ACTTC**GGC**ATTG-3′), using the Fd-GOGAT gene cloned from the genomic DNA of *L. boryana* as a template (Okuhara *et al.*, 1999), and was digested with *Afl*III and *Bgl*I, restriction sites for which were present in the primers. The DNA fragment encoding the remaining C-terminal part of the enzyme was excised from the gene by digestion with *Bgl*I and *Bam*HI. The two DNA fragments were simultaneously ligated into the *Nco*I/*Bam*HI cloning sites of pQE60 vector (Agilent Technologies). *Escherichia coli* JM105 cells transformed with the expression plasmid were cultivated in 2YT medium at 310 K. For induction of Fd-GOGAT, 0.1 m*M* IPTG was added to the culture medium at the early log phase. After induction, the bacterial cells were grown further overnight and harvested by centrifugation. The cell pellets were suspended in 50 m*M* Tris–HCl pH 7.5, 200 m*M* NaCl, 1 m*M* EDTA, 1 m*M* $MgCl_2$, 1 m*M* 2-OG, 0.5%(*v*/*v*) β-mercaptoethanol, 0.5 m*M* PMSF, disrupted by ultrasonic irradiation and centrifuged. The resulting supernatant was mixed with pre-swollen DE-52 (Whatman) in a batchwise manner and filtered. The flowthrough fraction containing Fd-GOGAT was diluted fivefold with 50 m*M* Tris–HCl pH 7.5, 1 m*M* 2-OG and applied onto a column of DE-52 equilibrated with the same buffer. Fd-GOGAT was bound to the column and eluted with 500 m*M* NaCl in the same buffer. Fd-GOGAT was further purified by affinity chromatography on a column of Fd-immobilized Sepharose 4B, which was developed with a linear gradient of 0–1 *M* NaCl in the same buffer. The concentrations of Fd and Fd-GOGAT were determined spectrophotometrically using molar extinction coefficients of 9.7 mM^{-1} cm^{-1} at 422 nm and 29.4 mM^{-1} cm^{-1} at 438 nm, respectively.

2.2. Crystallization

Purified Fd and Fd-GOGAT proteins were dialyzed against the initial crystallization buffer (50 m*M* Tris–HCl pH 7.5, 100 m*M* NaCl, 2 m*M* 2-OG). Crystallization screening was performed with Crystal Screen, Crystal Screen 2, Crystal Screen Cryo and Crystal Screen Lite (Hampton Research, Aliso Viejo, California, USA) using the hanging-drop vapour-diffusion method at 277 and 293 K. The volume of the reservoir solution was 150 µl and the droplets consisted of 2 µl each of the protein and reservoir solutions. Protein samples for crystallization were prepared by mixing Fd and Fd-GOGAT in 1:1, 2:1 and 3:1 molar ratios. Various protein concentrations (10–60 mg ml^{-1}) were also screened. Crystals were obtained in two weeks at 277 and 293 K using condition No. 22 of Crystal Screen Cryo [170 m*M* sodium

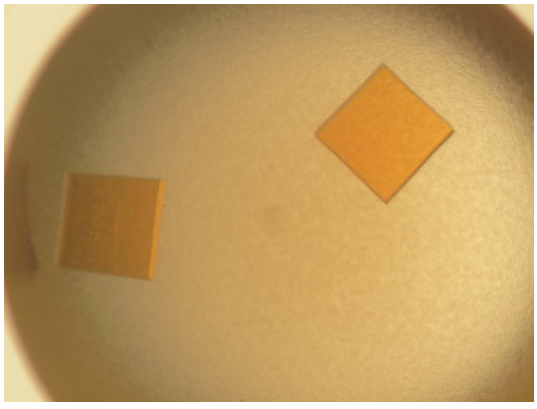

Figure 1
Typical crystals of the complex of Fd and Fd-GOGAT.

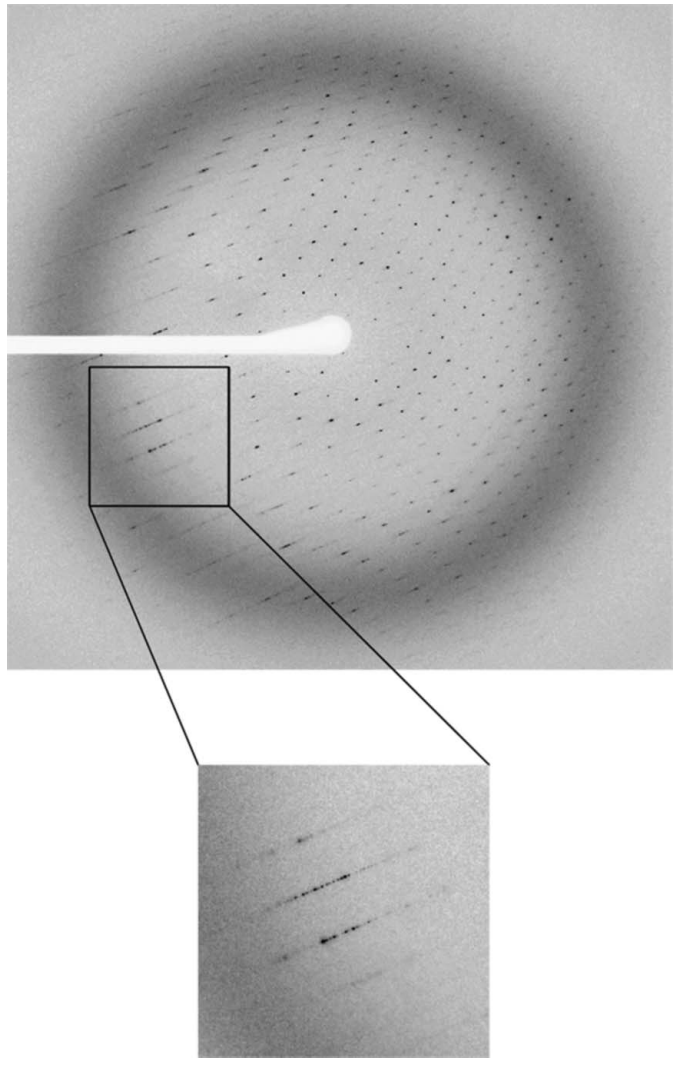

Figure 2
X-ray diffraction image from a crystal of the complex of Fd and Fd-GOGAT.

acetate trihydrate, 85 m*M* Tris–HCl pH 8.5, 25.5%(*w*/*v*) PEG 4000, 15%(*v*/*v*) glycerol]. After optimization of the crystallization condition, reddish-brown crystals could be reproducibly obtained from a solution consisting of equal volumes of 10 mg ml^{-1} protein solution containing a 2:1 ratio of Fd and Fd-GOGAT (50 m*M* Tris–HCl pH 8.2, 100 m*M* NaCl, 2 m*M* 2-OG, 2 m*M* azaserine) and precipitant solution [22–23%(*w*/*v*) PEG 3350, 170 m*M* sodium acetate trihydrate pH 7.0, 85 m*M* Tris–HCl pH 8.2, 15%(*v*/*v*) glycerol] at 277 K (Fig. 1). The crystals were plate-shaped, with maximum dimensions of 0.5 × 0.5 × 0.2 mm.

2.3. X-ray diffraction, data collection and processing

Crystals were mounted in a nylon loop with an adjustable metal tube and flash-cooled in liquid nitrogen. Native diffraction data were collected from a single frozen crystal on the BL44XU beamline at the SPring-8 synchrotron facility (Harima, Hyogo, Japan). Diffraction images were collected at 100 K using an MX225HE CCD detector (Rayonix, Illinois, USA) equipped with a Helix Technology cryosystem (Cryo Industries of America, New Hampshire, USA) (Fig. 2). In order to avoid spatial overlap of diffraction spots along the *c* axis, an adjustable metal tube at the base of the nylon loop was physically bent to an angle of approximately 75°. A data set consisting of a total of 1070 images was recorded with an oscillation range of 0.1° and an exposure time of 0.4 s per image. All diffraction data were processed and scaled with the *HKL*-2000 program package (Otwinowski & Minor, 1997). The data-collection statistics are summarized in Table 1.

Table 1
Data-collection statistics.

Values in parentheses are for the highest resolution shell.

X-ray source	BL44XU, SPring-8
Space group	$P4_3$
Unit-cell parameters (Å)	$a = b = 84.95$, $c = 476.31$
Wavelength (Å)	0.90000
Detector	MX225HE
Crystal-to-detector distance (mm)	270
Rotation range per image (°)	0.1
Total rotation range (°)	107
Exposure time per image (s)	0.4
Resolution range (Å)	50–2.65 (2.70–2.65)
Total reflections	361165
Unique reflections	96060
Completeness (%)	98.7 (100.0)
$R_{\rm merge}(I)$† (%)	0.086 (0.514)
$\langle I/\sigma(I)\rangle$	14.655 (2.671)
Multiplicity	3.8
Overall *B* factor from Wilson plot (Å^2)	49.9

† $R_{\rm merge}(I) = \sum_{hkl}\sum_i |I_i(hkl) - \langle I(hkl)\rangle| / \sum_{hkl}\sum_i I_i(hkl)$, where $I_i(hkl)$ is the intensity of the *i*th observation of reflection *hkl* and $\langle I(hkl)\rangle$ is the average intensity of reflection *hkl*.

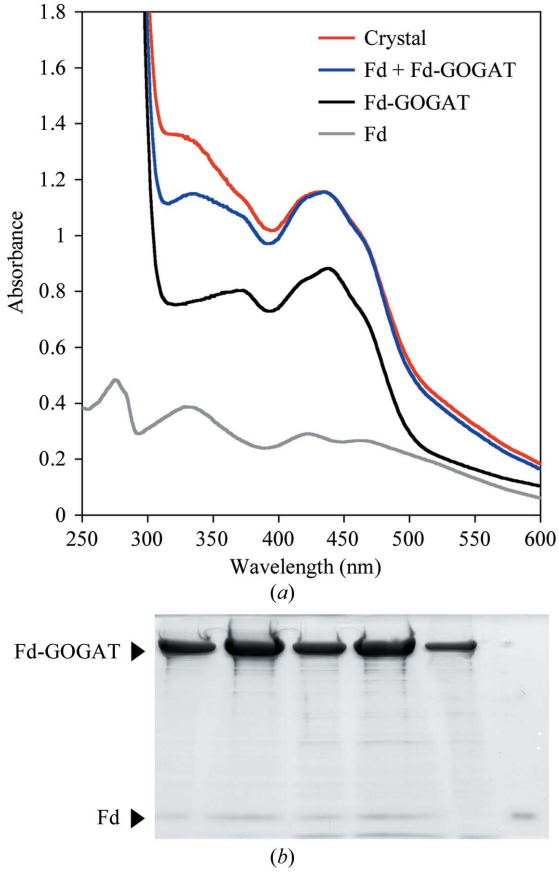

Figure 3
Protein analysis of the crystals of the complex between Fd and Fd-GOGAT. (*a*) Absorption spectra of 30 µ*M* Fd (grey line), 30 µ*M* Fd-GOGAT (black line), a mixture of 30 µ*M* Fd and 30 µ*M* Fd-GOGAT (blue line) and solubilized crystals (red line). (*b*) SDS–PAGE (10% gel) of the solubilized crystals. Lanes 1 and 2, 5 and 10 µg solubilized crystal protein, respectively; lane 3 and 4, 5 and 10 µg equimolar mixture of Fd and Fd-GOGAT, respectively; lane 5, 2 µg Fd-GOGAT; lane 6, 0.5 µg Fd.

3. Results and discussion

The coexistence of Fd and Fd-GOGAT in the crystals was confirmed by the absorption spectra and SDS–PAGE analysis (Fig. 3). The absorption spectra of dissolved crystals were similar to that of a mixture of Fd and Fd-GOGAT containing equal molar amounts (Fig. 3*a*). SDS–PAGE of the crystals yielded two significant bands with gel mobilities corresponding to those of Fd-GOGAT and Fd (Fig. 3*b*), indicating that the crystals contained a protein–protein complex composed of Fd and Fd-GOGAT.

The crystals belonged to the tetragonal space group $P4_1$ or $P4_3$, with unit-cell parameters $a = b = 84.95$, $c = 476.31$ Å. The $V_{\rm M}$ value of 2.50 Å^3 Da^{-1} indicated that the crystal contained two molecules of the complex of Fd and Fd-GOGAT per asymmetric unit. To obtain phase information, we carried out molecular replacement with the program *MOLREP* from the *CCP*4 program suite (Winn *et al.*, 2011). The search model for the molecular-replacement calculation was the structure of Fd-GOGAT from *Synechocystis* sp. PCC 6803 (PDB entry 1ofd; van den Heuvel *et al.*, 2003), which has 68% similarity to *L. boryana* Fd-GOGAT. The molecular-replacement calculation showed a unique solution for two Fd-GOGAT molecules in the asymmetric unit, indicating that the space group is $P4_3$. A difference Fourier map calculated using the structure factors and preliminary phase angles calculated from initial search models showed globular density corresponding to stoichiometric Fd molecules. Efforts towards final structure determination are currently in progress.

We thank E. Yamashita, A. Higashiura, T. Tsukihara and A. Nakagawa of the BL-44XU beamline at SPring-8 for their support during X-ray data collection (proposal No. 2011B6500). The MX225HE CCD detector (Rayonix) at BL44XU was supported financially by Academia Sinica and the National Synchrotron Radiation Research Center (Taiwan). This work was supported by Grant-in-Aids for Scientific Research (NM, TH and GK) from the Ministry of Education, Culture, Sports, Science and Technology of Japan and by the Funding Program for Next-Generation World-Leading Research

(GK) initiated by the Council for Science and Technology Policy of Japan.

References

Binda, C., Bossi, R. T., Wakatsuki, S., Arzt, S., Coda, A., Curti, B., Vanoni, M. A. & Mattevi, A. (2000). *Structure*, **8**, 1299–1308.
Dai, S., Friemann, R., Glauser, D. A., Bourquin, F., Manieri, W., Schürmann, P. & Eklund, H. (2007). *Nature (London)*, **448**, 92–96.
Hase, T., Schürmann, P. & Knaff, D. B. (2006). *Photosystem I. The Light-Driven Plastocyanin: Ferredoxin Oxidoreductase*, edited by J. H. Golbeck, pp. 477–498. Dordrecht: Springer.
Heuvel, R. H. H. van den, Ferrari, D., Bossi, R. T., Ravasio, S., Curti, B., Vanoni, M. A., Florencio, F. J. & Mattevi, A. (2002). *J. Biol. Chem.* **277**, 24579–24583.
Heuvel, R. H. H. van den, Svergun, D. I., Petoukhov, M. V., Coda, A., Curti, B., Ravasio, S., Vanoni, M. A. & Mattevi, A. (2003). *J. Mol. Biol.* **330**, 113–128.
Kimata-Ariga, Y., Matsumura, T., Kada, S., Fujimoto, H., Fujita, Y., Endo, T., Mano, J., Sato, F. & Hase, T. (2000). *EMBO J.* **19**, 5041–5050.
Kurisu, G., Kusunoki, M., Katoh, E., Yamazaki, T., Teshima, K., Onda, Y., Kimata-Ariga, Y. & Hase, T. (2001). *Nature Struct. Biol.* **8**, 117–121.
Matsumura, T., Kimata-Ariga, Y., Sakakibara, H., Sugiyama, T., Murata, H., Takao, T., Shimonishi, Y. & Hase, T. (1999). *Plant Physiol.* **119**, 481–488.
Okuhara, H., Matsumura, T., Fujita, Y. & Hase, T. (1999). *Plant Physiol.* **120**, 33–42.
Otwinowski, Z. & Minor, W. (1997). *Methods Enzymol.* **276**, 307–326.
Saitoh, T., Ikegami, T., Nakayama, M., Teshima, K., Akutsu, H. & Hase, T. (2006). *J. Biol. Chem.* **281**, 10482–10488.
Sakakibara, Y., Kimura, H., Iwamura, A., Saitoh, T., Ikegami, T., Kurisu, G. & Hase, T. (2012). In the press.
Suzuki, A. & Knaff, D. B. (2005). *Photosynth. Res.* **83**, 191–217.
Vanoni, M. A., Dossena, L., van den Heuvel, R. H. H. & Curti, B. (2005). *Photosynth. Res.* **83**, 219–238.
Winn, M. D. *et al.* (2011). *Acta Cryst.* D**67**, 235–242.